

# Magnetic property of $\text{Mn}_3\text{O}_4$ nanowires prepared by electrospinning

Z. W. MA<sup>\*</sup>, J. G. ZHAO<sup>a</sup>, Z. X. ZHANG<sup>b</sup>, Y. R. SU<sup>b</sup>, E. Q. XIE<sup>b</sup>

*Department of Physics and Electronic Engineering, Yuncheng University, Yuncheng, 044000, P.R. China*

*<sup>a</sup>College of Physics and Electronic Information, Luoyang Normal College, Luoyang, 471022, P.R. China*

*<sup>b</sup>School of Physical Science and Technology, Lanzhou University, Lanzhou, 730000, P.R. China*

$\text{Mn}_3\text{O}_4$  nanowires were prepared by electrospinning followed by  $\text{H}_2$  reduction. XRD patterns showed the samples were tetragonal phase with the average grain size of about 24.7 nm. The diameter of  $\text{Mn}_3\text{O}_4$  nanowires was about 100 nm and the nanowires were porous ones. The magnetic properties of the samples presented obvious the feature of ferromagnetism at 5 K and a small coercivity. The porous and magnetic features make that the nanowires can be used as the filtration for the separation of the magnetic-active particles.

(Received January 5, 2013; accepted July 11, 2013)

**Keywords:**  $\text{Mn}_3\text{O}_4$ , Nanowire, Electrospinning, Magnetic properties

## 1. Introduction

Manganese has many oxidation states and can form many different oxides, such as  $\text{MnO}$ ,  $\text{Mn}_3\text{O}_4$ ,  $\text{Mn}_2\text{O}_3$ ,  $\text{Mn}_5\text{O}_8$  and  $\text{MnO}_2$ , so it has tremendous potential in wide range of technical applications – catalysis, electrode materials, molecular adsorptions, gas-sensing devices, magnetic storage media, solar energy conversion, etc. [1-6]. Among them, the hausmannite phase,  $\text{Mn}_3\text{O}_4$  is one of the most stable oxides of manganese and possesses the ferromagnetism and electrochromic properties [7-9]. In particular, materials fabricated on a nanoscale can exhibit better phonon, optical, magnetic, thermal, and electrical properties than bulk materials. A number of methods were reported to fabricate nanostructured  $\text{Mn}_3\text{O}_4$ , for example, thermal decomposition, mild solution method, hydrothermal process,  $\gamma$ -ray irradiation, and so on [9-13]. Electrospinning is the most attractive because of its convenience, simplicity, and low cost in very recent years, which can also spin a variety of one-dimension materials at micro- and even nanoscale [14-16].

In this paper,  $\text{Mn}_3\text{O}_4$  nanowires are prepared by electrospinning method. The structure and magnetic properties have been characterized by X-ray diffraction (XRD), field emission scanning electron microscopy (FE-SEM) and superconducting quantum interference device (SQUID).

## 2. Experimental

In the first step, 0.5 g Manganese acetate ( $\text{C}_4\text{H}_6\text{MnO}_4 \cdot 4\text{H}_2\text{O}$ ) (analytical reagent, > 98%) was dissolved into 2 ml Deionized water by magnetic stirring 5

minutes. Second, 0.17 g Polyvinyl Alcohol (PVA) was added to this solution, followed by magnetic stirring for about 1 h. The mixed solution was loaded into a syringe equipped with a stainless needle with the diameter of 0.6 mm. A stainless steel grid plate was used to collect the electrospun nanowires. The distance between the tip of the needle and the collector is 20 cm. Upon applying a high voltage of 20 kV to the needle, a fluid jet ejected. The solvent evaporated and the charged nanowires were deposited on the collector. After dried by leaving in air for ~24 h, the collected nanowires were annealed at 450 °C for 4 h in air. Finally, the nanowires were annealed in  $\text{H}_2$  atmosphere at the pressure of 160 Pa and at the temperature of 600 °C for 6 h.

The structure of the samples was characterized by X-ray diffraction (XRD) (Philips, Regiku D/max-IIIIC) using  $\text{Cu K}\alpha$  ray (wavelength 1.5404 nm) at the grazing incidence angle of 1°. Field emission scanning electron microscopy (FESEM) (Hitachi, S-4800) was utilized to observe the morphology of the samples. Variable-temperature magnetization measurements under a magnetic field of 200 Oe and under both zero-field-cooled (ZFC) and field-cooled (FC) conditions were performed on a Quantum Design SQUID MPMS XL-7 (SQUID) from 300 K down to 5 K. The dc hysteresis loops were collected on the same SQUID in magnetic fields from 50000 to -50000 Oe at 5 K.

## 3. Results and discussion

Fig. 1 shows XRD patterns of the samples before annealed in  $\text{H}_2$  atmosphere. All observed peaks agree very well with JCPDS file 76-0150 and reveals that the sample

presents a cubic phase  $Mn_2O_3$ . The average grain size of  $Mn_2O_3$  nanowires estimated by Scherrer formula is about 18.8 nm. After high temperature  $H_2$  reduction, the sample presents a tetragonal phase  $Mn_3O_4$  (hausmannite structure) with the lattice constants of  $a = 5.760 \text{ \AA}$  and  $c = 9.444 \text{ \AA}$ , and seems also to contain a little amorphous phase, as shown in Fig. 2. The result is consistent with other results [1, 9] and the values of the bulk materials (JCPDS card #24-0734). The average size of the grains is about 24.7 nm. There is obviously no metallic phase in the samples after a long time reduction, so it can be inferred that  $Mn_3O_4$  is very stable and can be applied in harsh environment. In addition, although the O content in the sample reduces, the grain instead grows. It implied that the re-crystallization happens during the  $H_2$  reduction.

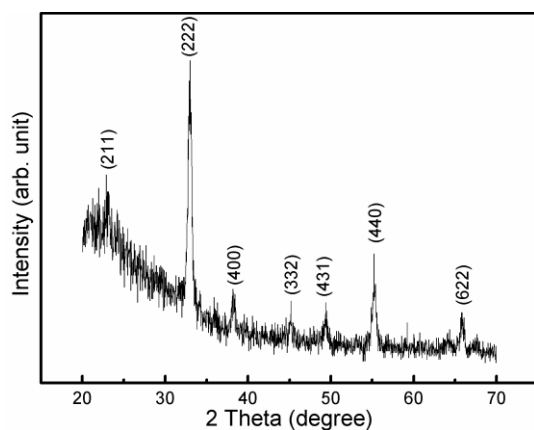


Fig. 1. XRD patterns of  $Mn_2O_3$  nanowires.

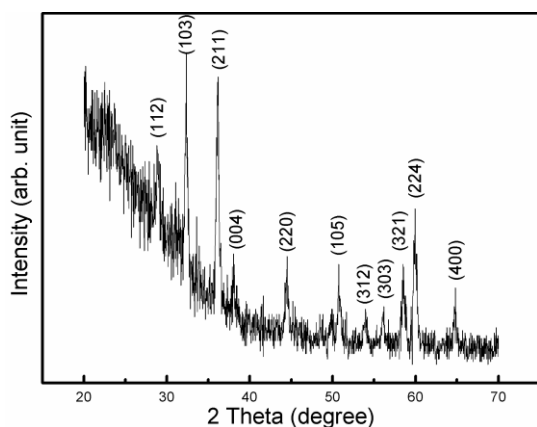


Fig. 2. XRD patterns of  $Mn_3O_4$  nanowires.

FESEM image of  $Mn_3O_4$  nanowires is shown in Fig. 3. It can be seen that  $Mn_3O_4$  nanowires are not very compact and porous, and the surface is not smooth. The nanowires are straight and about 100 nm in diameter. This morphology may be related to the evaporation of the solvents, the decomposing and removing of the organic phase via calcinations, the oxygen escape and the re-crystallization in the high temperature  $H_2$  reduction. The porous structure can increase the surface area of

$Mn_3O_4$  nanowires. Increasing of surface area is favor to many applications, such as absorption, filtration, catalysis, fuel cells, and solar cells [17].

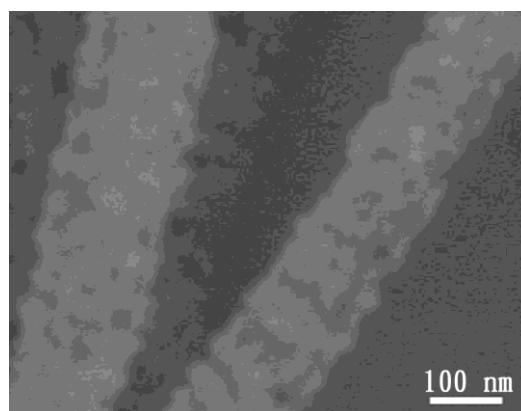


Fig. 3. FESEM image of  $Mn_3O_4$  nanowires.

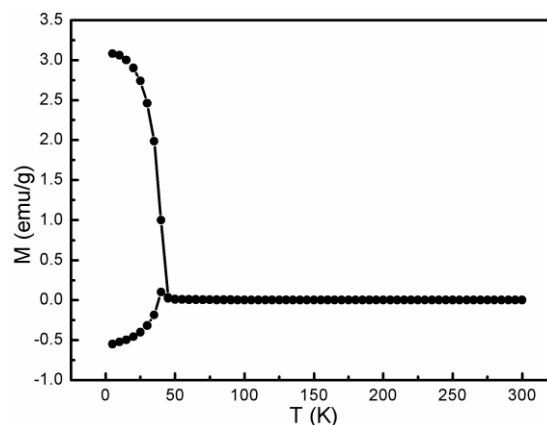


Fig. 4. ZFC-FC curve of  $Mn_3O_4$  nanowires at 200 Oe.

M-T curves of  $Mn_3O_4$  nanowires were measured in field cooled (FC) and zero field cooled (ZFC) conditions with an external field of 200 Oe, as shown in Fig. 4. The curve indicates that the FC curve exhibits an obvious deviation from the ZFC curve until 40 K, revealing that the Curie temperature ( $T_c$ ) of the sample is 40 K. This value is close to the bulk value of  $Mn_3O_4$ . In the FC measurements, the magnetization shows weak temperature dependence at lower temperature and obviously decreases until reaching the  $T_c$ . In contrast, the ZFC results show low magnetization in the low temperature region but increases obviously at a certain temperature. This special temperature matches  $T_c$  at a low external field. From Fig. 4, it can be known that the individual  $Mn_3O_4$  nanowires is paramagnetic at room temperature, and exhibit ferromagnetic under 40 K. Fig. 5 shows the representative hysteresis curve of  $Mn_3O_4$  nanowires at 5 K, which shows the coercivity of  $Mn_3O_4$  nanowires is 33.6 Oe and the saturation magnetization of the sample is 4.92 emu/g. The saturation magnetization is smaller than the single crystal

Mn<sub>3</sub>O<sub>4</sub> nanowires [18]. This can be ascribed to the Mn<sub>3</sub>O<sub>4</sub> nanowires prepared by electrospinning method is polycrystalline and porous ones, and the crystal boundary and other defect make the saturation magnetization smaller than the single crystal samples. This result also indicates the ferromagnetic property of Mn<sub>3</sub>O<sub>4</sub> nanowires at low temperature. The porous and magnetic features of the sample make that they can be used as the filtration to separate effectively the magnetic-active particle through the application of an external magnetic field [17].

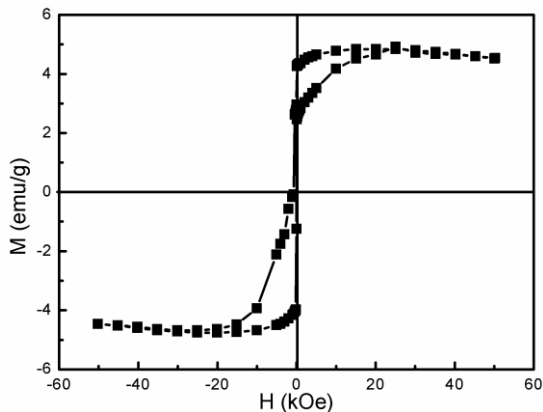


Fig. 5. *M-H curve of Mn<sub>3</sub>O<sub>4</sub> nanowires at 5 K.*

#### 4. Conclusion

In summary, Mn<sub>2</sub>O<sub>3</sub> nanowires were prepared by the electrospinning method followed by annealing in air. After the further H<sub>2</sub> reduction, Mn<sub>3</sub>O<sub>4</sub> nanowires were obtained. Mn<sub>3</sub>O<sub>4</sub> nanowires were tetragonal phase with a diameter of about 100 nm. The samples were porous, which make them have many potential application. The magnetic properties of the samples were measured by SQUID and presented obviously ferromagnetic at the low temperature.

#### Acknowledgements

This work was supported by the doctor starting fund of Yuncheng University (YQ-2011036).

#### References

- [1] P. Zhang, Y. Zhan, B. Cai, C. Hao, J. Wang, C. Liu, Z. Meng, Z. Yin, Q. Chen, *Nano Res.* **3**, 235 (2010).
- [2] Y. F. Han, F. X. Chen, Z. Y. Zhong, K. Ramesh, L. W. Chen, E. Widjaja, *J. Phys. Chem. B* **110**, 24450 (2006).
- [3] A. E. Fischer, K. A. Pettigrew, D. R. Rolison, R. M. Stroud, J. W. Long, *Nano Lett.* **7**, 281 (2007).
- [4] L. Liu, H. Liang, H. Yang, J. Wei, Y. Yang, *Nanotechnology* **22**, 015603 (2011).
- [5] J. Liu, J. Essner, J. Li, *Chem. Mater.* **22**, 5022 (2010).
- [6] Z. H. Wang, D. Y. Geng, W. J. Hu, W. J. Ren, Z. D. Zhang, *J. Appl. Phys.* **105**, 07A315 (2009).
- [7] A. E. Berkowitz, G. F. Rodriguez, J. I. Hong, K. An, T. Hyeon, N. Agarwal, D. J. Smith, E. E. Fullerton, *Phys. Rev. B* **77**, 024403 (2008).
- [8] T. Maruyama, Y. Osaki, *J. Electrochem. Soc.* **142**, 3137 (1995).
- [9] S. Thota, B. Prasad, J. Kumar, *Mater. Sci. Eng. B* **167**, 153 (2010).
- [10] W. Chen, N. Wang, L. Liu, Y. Cui, X. Cao, Q. Chen, L. Guo, *Nanotechnology* **20**, 445601 (2009).
- [11] X. Fang, X. Lu, X. Guo, Y. Mao, Y. Hu, J. Wang, Z. Wang, F. Wu, H. Liu, L. Chen, *Electrochem. Commun.* **12**, 1520 (2010).
- [12] H. Dhaouadi, A. Madani, F. Touati, *Mater. Lett.* **64**, 2395 (2010).
- [13] Y. Hu, J. Chen, X. Xue, T. Li, *Mater. Lett.* **60**, 383 (2006).
- [14] S. V. Fridrikh, J. H. Yu, M. P. Brenner, G. C. Rutledge, *Phys. Rev. Lett.* **90**, 144502 (2003).
- [15] J. Zhao, H. Duan, Z. Ma, L. Liu, E. Xie, J. Optoelectron. *Adv. Mater.* **10**, 3029 (2008).
- [16] Y. Su, B. Lu, Y. Xie, Z. Ma, L. Liu, H. Zhao, J. Zhang, H. Duan, H. Zhang, J. Li, *Nanotechnology* **22**, 285609 (2011).
- [17] D. Li, Y. Xia, *Adv. Mater.* **16**, 1151 (2004).
- [18] S. Sambasivam, G. J. Li, J. H. Jeong, B. C. Choi, K. T. Lim, S. S. Kim, T. K. Song, *J. Nanopart. Res.* **14**, 1138 (2012).

\*Corresponding author: mazw06@gmail.com